AJNR

Assessment of the Deep Gray Nuclei in Holoprosencephaly

Erin M. Simon, Robert Hevner, Joseph D. Pinter, Nancy J. Clegg, Van S. Miller, Stephen L. Kinsman, Jin S. Hahn and A. James Barkovich

AJNR Am J Neuroradiol 2000, 21 (10) 1955-1961
http://www.ajnr.org/content/21/10/1955

AJNR Am J Neuroradiol 21:1955–1961, November/December 2000

Assessment of the Deep Gray Nuclei in Holoprosencephaly

Erin M. Simon, Robert Hevner, Joseph D. Pinter, Nancy J. Clegg, Van S. Miller, Stephen L. Kinsman, Jin S. Hahn, and A. James Barkovich

BACKGROUND AND PURPOSE: **Although holoprosencephaly has been known for many years, few detailed analyses have been performed in a large series of patients to outline the range of morphology in this disorder, particularly regarding the deep gray nuclear structures. We reviewed a large patient cohort to elucidate the combinations of morphologic aberrations of the deep gray nuclei and to correlate those findings with recent discoveries in embryology and developmental neurogenetics.**

METHODS: **A retrospective review of the imaging records of 57 patients (43 MR studies and 14 high-quality CT studies) to categorize the spectrum of deep gray nuclear malformations. The hypothalami, caudate nuclei, lentiform nuclei, thalami, and mesencephalon were graded as to their degree of noncleavage. Spatial orientation was also evaluated, as was the relationship of the basal ganglia to the diencephalic structures and mesencephalon. The extent of noncleavage of the various nuclei was then assessed for statistical association.**

RESULTS: **In every study on which it could be accurately assessed, we found some degree of hypothalamic noncleavage. Noncleavage was also common in the caudate nuclei (96%), lentiform nuclei (85%), and thalami (67%). Complete and partial noncleavage were more common in the caudate nuclei than in the lentiform nuclei. The degree of thalamic noncleavage was uniformly less than that in the caudate and lentiform nuclei. Abnormalities in alignment of the long axis of the thalamus were seen in 71% of cases, and were associated with degree of thalamic noncleavage; 27% of patients had some degree of mesencephalic noncleavage.**

CONCLUSION: **The hypothalamus and caudate nuclei are the most severely affected structures in holoprosencephaly, and the mesencephalic structures are more commonly involved than previously thought in this ''prosencephalic disorder.'' These findings suggest the lack of induction of the most rostral aspects of the embryonic floor plate as the cause of this disorder.**

Despite the vast amount of attention in the literature devoted to the complex facial malformations that often accompany the brain, parenchymal abnormalities in holoprosencephaly (HPE) (1–7), it is generally the profound brain anomalies that dominate the clinical picture and prognosis. Although the ''face predicts the brain'' in approximately 80% of cases (8, 9), the brain predicts the outcome in all patients.

The deep gray nuclear structures and diencephalon are profoundly affected in the vast majority of patients with HPE. To our knowledge, the specific morphologic abnormalities in these structures have not been studied in any formal fashion, as large postnatal patient cohorts are difficult to accumulate in this uncommon disorder, which affects 0.48 to 0.88 of the population per every 10,000 live births (7, 10, 11). We therefore undertook an investigation of the basal ganglia, diencephalon, and mesencephalon to assess their degree of involvement and interrelationships, and to correlate this data with the most up-to-date information regarding the genetic factors controlling early brain development. In the future, we hope to correlate the morphologic data with clinical and neurodevelopmental information

Received February 24, 2000; accepted after revision May 15.

From the Departments of Diagnostic Radiology (E.M.S., A.J.B.), and Psychiatry (R.H.), University of California, San Francisco; the Department of Neurology, Stanford University, Stanford, California (J.D.P., J.S.H.); the Department of Neurology, Texas Scottish Rite Hospital for Children, Dallas (N.J.C., V.S.M.); the Department of Neurology, Kennedy Krieger Institute, Baltimore (S.L.K.); and The Carter Centers for Brain Research in Holoprosencephaly and Related Malformations (E.M.S., R.H., J.D.P., N.J.C., V.S.M., S.L.K., J.S.H., A.J.B.).

Supported in part by The Carter Centers for Brain Research in Holoprosencephaly and Related Malformations, and by NIH grant K12 NSO1692 (J.D.P.).

Presented in part at the annual meeting of the American Society of Neuroradiology Annual Meeting, Atlanta, April 2000.

Address reprint requests to Erin M. Simon, MD, OTR, Department of Radiology, Division of Neuroradiology, L 358, University of California, San Francisco, 505 Parnassus Ave, Box 0628, San Francisco, CA. 94143.

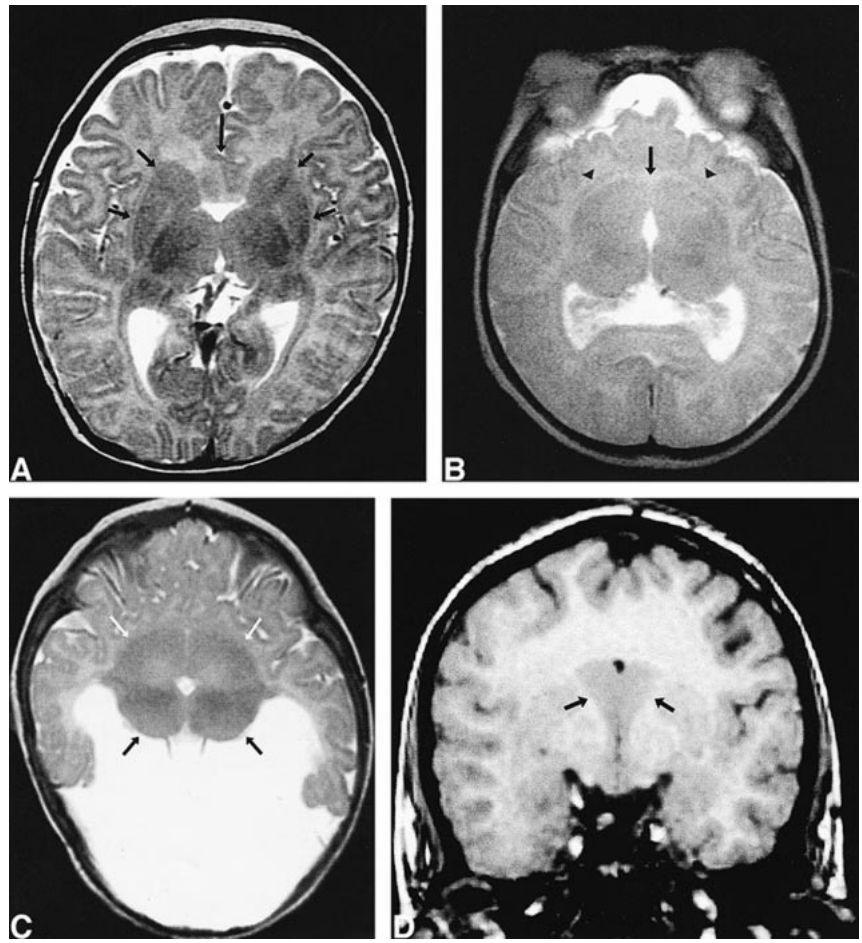

FIG 1. Range of noncleavage of the basal ganglia and thalamus.

A, Grade 0: Axial T2-weighted image at the level of the third ventricle shows the abnormally deep anterior IHF (*long arrow*) and widely separated caudate and lentiform nuclei (*short arrows*).

B, Grade 1: Axial T2-weighted image at the level of the third ventricle shows the medial location and small amount of contact between the caudate nuclei (*arrow*). Note also the noncleavage of the claustra (*arrowheads*) and probable anterior limbs of the internal capsules (white matter posterior to claustra).

C, Grade 2: Axial T2-weighted image in a more severely affected patient shows the partial noncleavage of the lentiform nuclei (*white arrows*) and thalami (*black arrows*).

D, Grade 3: Coronal 3D spoiled gradient-echo image through the caudate heads shows complete failure of cleavage (*arrows*).

to establish more accurate stratification measures for prediction of patient outcome.

Methods

The brain imaging studies were selected from patients referred to The Carter Centers for Brain Research in Holoprosencephaly and Related Malformations, a national consortium funded by a nonprofit private foundation, as well as from patients referred to the authors and their institutions. A total of 78 imaging studies were reviewed retrospectively by two neuroradiologists. Fourteen of these studies showed the middle interhemispheric variant of HPE, as described by Barkovich and Quint (12), and will be reported separately. Of the 64 remaining cases of ''classical'' HPE, 13 were alobar, 42 were semilobar, and nine were lobar, according to standard definitions (1, 2, 13).

Fifty-seven of the 64 studies that showed classical HPE were of adequate quality to assess the deep gray nuclei. Seven studies were eliminated because of motion artifacts, poor copy quality, or a section thickness more than 6 mm (too great to assess the deep structures). Of the remaining studies, 43 were MR images and 14 were CT scans. Patients ranged in age from 1 day to 15 years. Because the studies were performed at multiple institutions on a variety of machines, the imaging techniques varied considerably. All MR studies had sagittal T1-weighted sequences and at least one axial (T1- or T2-weighted) sequence. Coronal sequences were available in 30 patients. Paramagnetic contrast material was not administered. CT studies were performed only in the axial plane, without iodinated contrast; they were included in the study only if the section thickness was 5 mm or less.

The caudate nuclei, lentiform nuclei, thalami, and mesencephalon were graded on a scale from 0 to 3, with 0 = complete separation, 1 = less than 50% noncleavage or abnormal medial location, 2 = 50% to 99% noncleavage, and 3 = complete noncleavage (Fig 1). The degree of hypothalamic noncleavage was assessed using a scale of 0 to 2, with 0 = complete separation, 1 = partial (anterior) noncleavage, and 2 = complete noncleavage (Fig 2). When there was a single, deep gray nuclear mass, diminished in volume and without discernible separation, the case was considered grade 3 for the basal ganglia and thalami and grade 2 for the hypothalamus (Fig 3). Noncleavage among the basal ganglionic, thalamic, hypothalamic, and mesencephalic malformations was assessed for statistical association.

Three major categories of spatial orientation of the thalami were present in this patient population, as determined by the angulation of the long axes. Thalami with their long axis at an angle approximately 30° to 45° relative to the plane of the interhemispheric fissure (IHF) were graded 0 (essentially normal), those with their long axis in a largely anteroposterior direction (parallel to the plane of the IHF) were graded 1, and those oriented relatively perpendicular to the IHF were graded 2 (Fig 4). The association between spatial orientation and degree of noncleavage was also assessed statistically. All associations of noncleavage among the deep nuclei were tested for statistical significance using Fisher's exact test. A P value of less than .05 was considered significant.

Results

Raw data are summarized in the Table. In every study in which it could be accurately assessed,

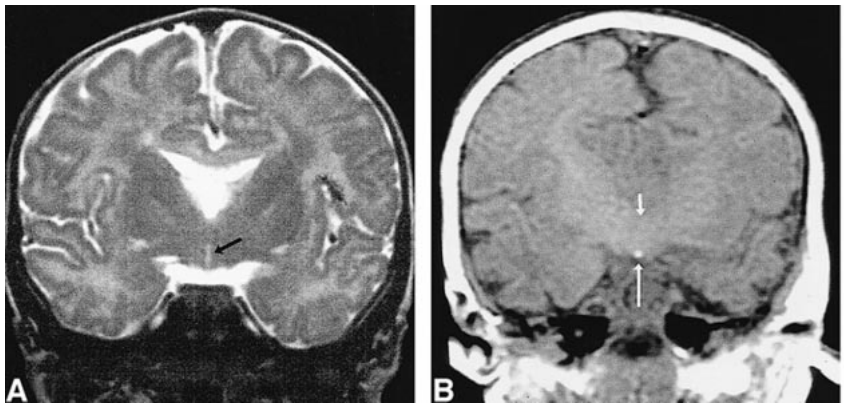

FIG 2. Range of noncleavage of the hypothalamus.

A, Grade 1: Coronal T2-weighted image shows the attenuated anterior recess of the third ventricle (*arrow*) in the setting of partial hypothalamic noncleavage.

B, Grade 2: Coronal T1-weighted image shows the continuity of the hypothalamus across the midline of the basal forebrain (*short arrow*). Note the associated ectopic neurohypophysis (*long arrow*).

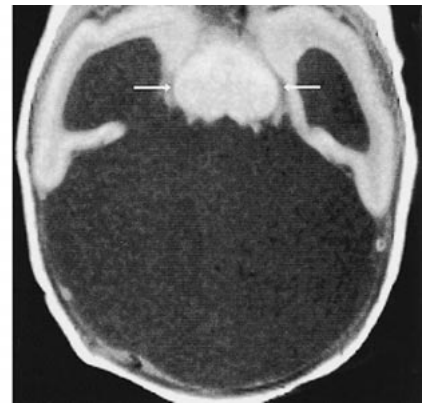

FIG 3. Deep gray nuclear mass. Axial T1-weighted image shows the noncleaved deep gray nuclear mass, which is diminished in volume and without discernible structures (*arrows*).

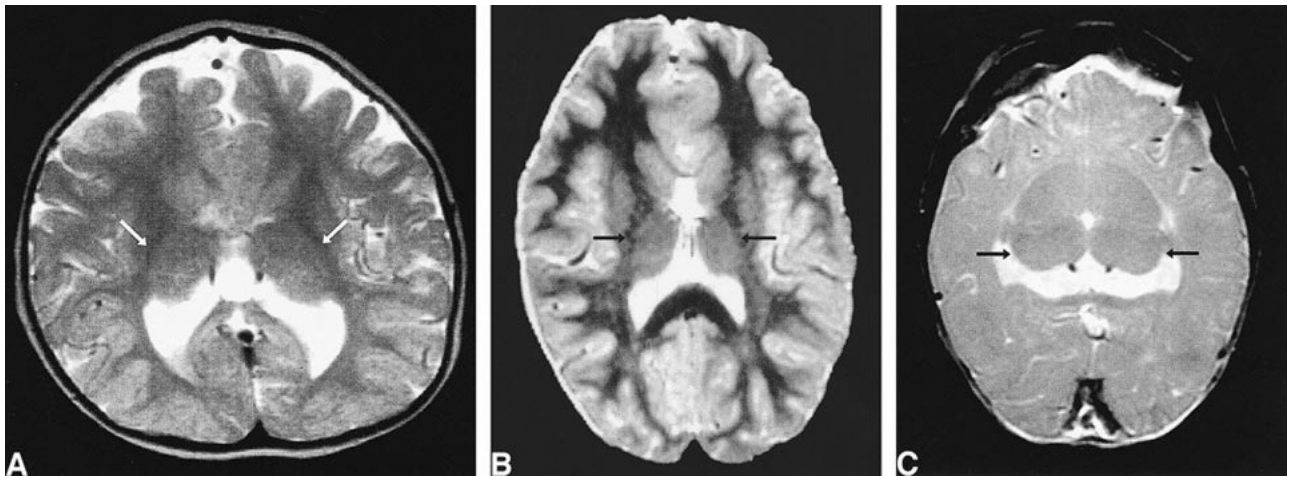

FIG 4. Spatial orientation of the thalami.

A, Grade 0: Axial T2-weighted image shows the thalami with their long axes at an angle approximately 30° to 45° relative to the plane of the IHF (*arrows*).

B, Grade 1: Axial T2-weighted image shows the thalami with their long axes approximately parallel to the plane of the IHF (*arrows*).

C, Grade 2: Axial T2-weighted image shows the thalami with their long axes approximately perpendicular to the plane of the IHF (*arrows*).

Grading of deep structural noncleavage

	Total No. of Cases (CT/MR)				
Structure	Total Assessed	Grade 0	Grade 1	Grade 2	Grade 3
Hypothalamus	56 (13/43)	0 (0/0)	18 (5/13)	38 (8/30)	· · ·
Caudate nucleus	56 (14/42)	2 (1/1)	11 (2/9)	7 (3/4)	36 (8/28)
Lentiform nucleus	55 (14/41)	8 (2/6)	13 (4/9)	13 (1/12)	21 (7/14)
Thalamus	57 (14/43)	19 (4/15)	12 (2/10)	11 (2/9)	15 (6/9)
Thalamic orientation*	49 (10/39)	14 (2/12)	3 (1/2)	32 (7/25)	· · ·
Mesencephalon	51 (8/43)	37 (2/35)	3 (0/3)	2 (0/2)	9 (6/3)

Note.—Grade 0 indicates complete separation; grade 1, minimal noncleavage or medial deviation; grade 2, partial noncleavage; grade 3, total noncleavage; the hypothalamus was graded on a 0–2 scale.

* Grade 0, approximately 30–45° angle relative to interhemispheric fissure (IHF); grade 1, relatively parallel to IHF; grade 2, relatively perpendicular to IHF.

there was some degree of hypothalamic noncleavage (56/56 cases, 100%). Some degree of caudate noncleavage was found in 54 (96%) of 56 cases, and in six cases (11%) there was a single deep gray nuclear mass. Complete and partial noncleavage were more common in the caudate nuclei than in the lentiform nuclei ($P < .0005$). The lentiform nuclei were completely separated in eight (15%) of the 55 cases in which they could be accurately evaluated, with the remaining 85% showing some noncleavage. Determining the exact extent of lentiform separation was sometimes troublesome owing to the difficulty in distinguishing the lentiform nuclei from the caudate nuclei on axial images.

Noncleavage of the thalami could be accurately assessed in all cases and was less common, occurring in 38 patients (67%). The grade of noncleavage was less than or equal to that seen in the caudate ($P < .0005$) and lentiform ($P < .0005$) nuclei.

Abnormalities in orientation of the long axis of the thalamus were seen in 35 (71%) of the 49 cases in which it could be assessed, and were associated with the degree of thalamic noncleavage (MR studies, $P = .0001$; CT studies, $P = .33$; overall, $P = .0004$). There was no association between hypothalamic, caudate, or lentiform noncleavage and thalamic orientation.

Fourteen (27%) of 51 studies showed some degree of mesencephalic noncleavage, which was associated with the presence of thalamic noncleavage (MR studies, $P = .08$; CT studies, $P = .25$; overall, $P = .0002$) but not with the degree of abnormal thalamic orientation.

Discussion

Advances in modern medicine have enabled patients with brain malformations to survive infancy, often into late childhood or adulthood. Therefore, it is useful to be able to prognosticate developmental potential of affected infants to better prepare caregivers and parents for the future needs of their child.

Although HPEs are typically classified according to the system of DeMyer and coworkers (1, 2) into alobar, semilobar, and lobar forms, it has become apparent that several important features, such as cortical malformations and variations in separation of deep gray nuclei, cannot be incorporated into this classification scheme; therefore, neurodevelopmental outcome cannot always be predicted accurately by this rather inflexible system (1–3, 8–10, 13–15). For example, our study included a patient whose disorder would have been classified as semilobar HPE by the DeMyer classification, but the patient was severely retarded as a result of an accompanying large cortical malformation. The purpose of this study was to examine the morphology of the basal ganglia in a large series of patients with HPE as a first step in formulating a more sophisticated algorithm for neurodevelopmental prognostication. We suggest that the flexibility of this new classification scheme, which is based on more detailed morphologic analyses, will allow for more precise predictions of developmental outcome.

This study is also the most detailed morphologic analysis of the deep gray nuclei to date in a cohort of patients with HPE. Our results confirm some of those reported in the literature, but are in disagreement with others. Probst (3) has reported ''hypoplastic. . . corpora striata [and] thalamic nuclei''; others have indicated small or frankly absent deep gray nuclei (15, 16). Without the benefit of volumetric imaging in all cases of this retrospective series, we could not accurately assess the volume of the involved structures, although they were clearly diminutive, or even absent, in the more severely affected cases. This may be the subject of future investigation by members of our group. One interpretation of the thalamic orientation is that certain thalamic nuclei could be hypoplastic or absent, resulting in an apparent malalignment of the long axis. Our subjective impression is that, in the majority of cases, the overall volume of the thalami is not significantly diminished, although this has not been established objectively.

The recent review by Golden (14) also indicates that the degree of involvement of the basal ganglia and thalami is ''frequently in direct proportion to the severity of the cerebral hemispheric malformation.'' While our series generally concurs with these findings, we encountered cases with alobar or severe semilobar HPE and little or no lentiform (3/26) or thalamic (7/26) involvement (grades 1 or 0). This is contrary to older reports, in which the basal ganglia and thalami were always noncleaved in the more severe cases (3, 8, 9). Our observations also concur with those noted by Golden (14) and others that in ''less severe forms. . . the head of the caudate is commonly fused.''

Analysis of the hypothalamus is notably absent from most morphologic descriptions in the HPE literature. This is particularly surprising given the universal finding of noncleavage in our series. The observation of uniform hypothalamic involvement is most likely the result of the high number of MR examinations in the current study; these provided the advantage of multiplanar analysis of the hypothalamus, often with thin sections. Many prior reports included gross and microscopic evaluation, which should provide highly accurate assessment of the hypothalamic involvement. However, the small size of the hypothalamus and the difficulty in sectioning unmyelinated neonatal brains may have contributed to the lack of detection of hypothalamic anomalies. It is also possible that the underreporting of hypothalamic anomalies reflects the relative emphasis on facial anomalies in the literature.

In several categories, the power of the findings on our CT scans was much less significant than the findings on our MR studies. We propose several possible explanations. First, fewer CT scans were available for review that provided adequate section

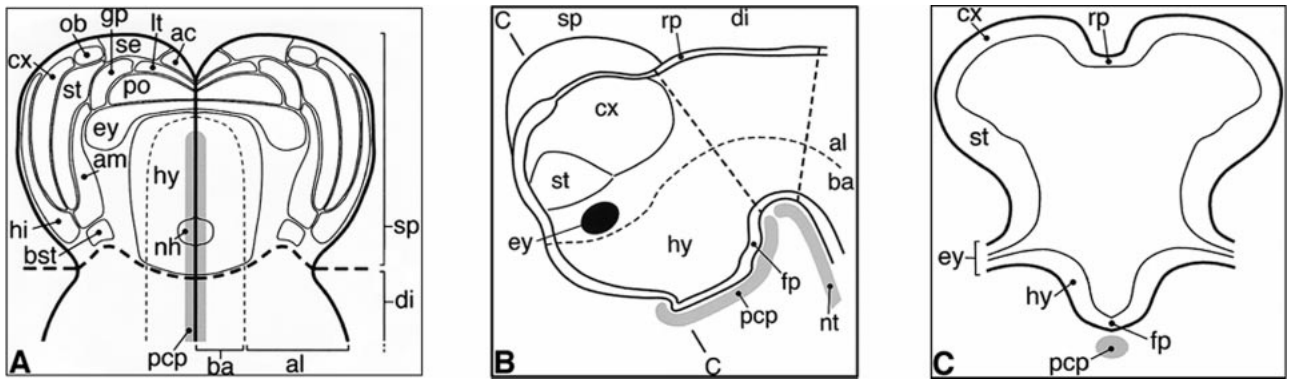

FIG 5. Diagrams of the developing prosencephalon.

A, Superior view of the neural plate, with the *top* being the rostral end at the anterior neuropore and the *bottom* being more caudal at the level of the diencephalon. Adapted from (25) with permission from the *Annual Review of Neuroscience,* Volume 21, 1998.

B, Lateral view of the neural plate, with the floor plate (*fp*) at the *bottom* and the roof plate (*rp*) at the *top.* Adapted from (24) with permission from The Company of Biologists, Ltd.

C, Coronal view of the neural plate with the roof plate (*rp*) (dorsal) at the *top* and the floor plate (*fp*) and prechordal plate (*pcp*) (ventral) at the *bottom.*

The more rostral and alar portion, superiorly (above the *horizontal dashed black line* in *A*) and to the left (anterior to the *vertical dashed black line* in *B*) is the secondary prosencephalon (*sp*) whereas the more inferior (in *A*) and right-sided portion (in *B*) is the diencephalon (*di*). The longitudinal *gray* area represents the prechordal plate. The *horseshoe-shaped dashed black line* surrounding the prechordal plate (in *A*) represents the boundary between the basal (or ventral) plate (*ba*) and the alar (or dorsal) plate (*al*). Within the secondary prosencephalon, structures at all dorsal and ventral levels are affected. The basal midline regions closest to the floor plate and to the lateral ventricles are the most severely affected in HPE. The reason for this is illustrated in *C.* In normal embryonic development, an interplay of dorsalizing molecules (emanating from the roof plate) and ventralizing molecules (emanating from the prechordal plate and floor plate) modulates regional identity of tissues along the dorsoventral axis of the neural tube. Either a lack of production of ventralizing factors or an overproduction of dorsalizing factors can result in noncleavage (commonly called fusion) of structures that normally lie just lateral to the midline. This is the presumed mechanism by which HPE develops. *nh* indicates neurohypophysis; *hy,* hypothalamus; *ey,* eyefields; *gp,* globus pallidus; *am,* amygdala; *ac,* anterior commissure; *lt,* laminal terminalis; *st,* striatum (caudate and putamen); *cx,* cortex; *hi,* hippocampus; *se,* septum; *po,* preoptic nucleus; *ob,* olfactory bulb; *bst,* bed nucleus of stria terminalis.

thickness and image quality for confident assessment of the deep structures, resulting in an intrinsically less powerful group. Second, the CT scans tended to represent a more severely affected patient population, as MR studies are more difficult to obtain in a critically ill child, particularly in the neonatal period, when many of these children are imaged. This hypothesis is supported by the fact that complete (grade 3) thalamic noncleavage was seen more commonly on the CT scans (6/4) than on the MR images (9/43). The relative lack of variation in the CT sample hampered the analysis, as having no patients or only one patient in several categories of comparison (ie, grade 2 for lentiform nucleus) potentially affects the statistical computations.

The anatomic spectrum of HPE reported here fits well with the proposed mechanisms of HPE pathogenesis based on recent studies in humans and animal models. These models have implicated defects of dorsoventral patterning in the pathogenesis of HPE. In normal embryonic development, the interplay between dorsalizing molecules (including bone morphogenetic proteins) and ventralizing molecules (chiefly the proteins encoded by the Sonic hedgehog [Shh] gene) modulates regional identity of tissues along the dorsoventral axis of the neural tube. This process is best understood in the spinal cord, where ventral identity is induced by Shh proteins secreted from the notochord, and dorsal identity is induced by bone morphogenetic proteins originating from nonneural ectoderm. The gradients of dorsal and ventral signaling molecules then induce distinct combinations of specific transcription factors in populations of cells at different dorsoventral levels. These transcription factors induce the formation of molecules that cause their cells to differentiate; those in the ventral neural tube become motor neurons and those in the dorsal neural tube become sensory relay neurons (17). A similar but more complicated process seems to be at work in the embryonic forebrain (18). The source of ventralizing signals for the forebrain appears to be the prechordal plate, a region of foregut mesenderm underlying the embryonic hypothalamus and thalamus. Like the notochord (which extends anteriorly only as far as the midbrain), the prechordal plate produces Shh proteins and induces the expression of ventral transcription factors. Mutations of the Shh gene have been linked to HPE in humans (19, 20) and in mice (21), indicating that HPE can be caused by a deficiency of ventral induction. An HPE-like malformation can also be caused by the implantation of beads coated with dorsalizing factors in embryonic chick brains (22). Thus, either insufficient ventralization or excessive dorsalization in early embryonic development can cause HPE.

Recently, studies of developmental gene expression (23, 24) and cell fate mapping (25) have shed new light on the organization and patterning of the embryonic forebrain, with important implications for understanding HPE (Fig 5). First, the position

of the dorsoventral boundary (equivalent to the alar-basal boundary in the developing spinal cord) has been localized within the hypothalamus (24). Therefore, the tuber cinereum, infundibulum, and mammillary bodies are ventral (basal) territories, whereas the optic chiasm, preoptic area, and telencephalic regions (including cortex, basal ganglia, and septum) lie within dorsal (alar) territories. Second, more accurate characterization of the longitudinal (segmental) organization of the forebrain along the anteroposterior axis (23, 25, 26) indicates that the hypothalamus is not part of the diencephalon, as classically conceived, but is grouped with the telencephalon in an anterior domain known as the secondary prosencephalon (Fig 5). Thus, the structures most consistently malformed in HPE (ie, the cortex, striatum, and hypothalamus) all belong to the same embryonic anteroposterior domain—the secondary prosencephalon—but occupy different dorsoventral positions within it. In this light, HPE may be best viewed as a disorder of dorsoventral patterning affecting the secondary prosencephalon. The primary defect may originate in patterning centers, such as the prechordal plate (14), or in the response of forebrain tissues to signal received from the patterning centers.

Among brain structures derived from the secondary prosencephalon, our results suggest that the frequency of noncleavage in HPE is dependent on proximity to the midline and to the ventricular system, which is also malformed in HPE. Structures normally located adjacent to the midline and/or ventricles (such as the cingulate cortex, caudate nucleus, and medial hypothalamus) are more frequently noncleaved than are structures normally located further from the midline or ventricles (such as the globus pallidus). This suggests a connection between dorsoventral patterning and growth or survival of cells along the midline (14). Also, the involvement of more posterior brain structures, such as the thalamus (diencephalon) and midbrain (mesencephalon), decreases with distance from the anterior pole. This gradient of involvement in HPE may be related to the relative effectiveness of ventralizing signals from the notochord and prechordal plate. Finally, much of the phenotypic variability in HPE is probably the result of genetic heterogeneity, because many genes participate in the production and transduction of ventralizing and dorsalizing signals. Indeed, it has already been shown that HPE can be caused by mutations of at least three different genes: Shh (20) ZIC2 (27), and SIX3 (28). Teratogenic influences must also be considered (29).

It is not clear whether mutations of specific genes result in specific morphologic characteristics in HPE. Correlations of the genotypes of our patients with the observed morphologic phenotypes are under way to explore this possibility.

Conclusion

The deep brain structures, including the mesencephalon, are more profoundly affected in HPE than previously thought. Seemingly underappreciated in previous reports, the hypothalamus and caudate nuclei are the most severely affected structures. Abnormalities in structural orientation of the thalami are associated with degree of noncleavage. These patterns of deep gray nuclear involvement suggest a lack of induction of the embryonic floor plate by prechordal mesenchyme and, perhaps, notochord. The patterns also provide evidence that the anlage of the hypothalamus and caudate nuclei are the most rostral structures in the developing neural plate. This analysis of the morphologic spectrum of HPE contributes to a better understanding of the embryologic and genetic factors influencing the embryonic floor plate and roof plate.

References

1. DeMyer W, Zeman W. **Alobar holoprosencephaly (arhinencephaly) with median cleft lip and palate: clinical, nosologic, and electroencephalographic considerations.** *Confin Neurol* 1963; 23:1–36
2. DeMyer W, Zeman W, Palmer CG. **The face predicts the brain: diagnostic significance of median facial anomalies for holoprosencephaly (arhinencephaly).** *Pediatrics* 1964;34:256–263
3. Probst FP. ***The Prosencephalies: Morphology, Neuroradiological Appearances and Differential Diagnosis.*** New York: Springer; 1979
4. Kobori JA, Herrick MK, Urich H. **Arhinencephaly: the spectrum of associated malformations.** *Brain* 1987;110:237–260
5. Sulik KK, Johnston MC. **Embryonic origin of holoprosencephaly: interrelationship of the developing brain and face.** *Scan Elec Microsc* 1982;260:309–322
6. Fitz CR. **Holoprosencephaly and related entities.** *Neuroradiology* 1983;25:225–238
7. Olsen CL, Hughes JP, Youngblood LG, Sharpe-Stimac M. **Epidemiology of holoprosencephaly and phenotypic characteristics of affected children: New York State, 1984–1989.** 1997;73: 217–226
8. Cohen MM, Sulik KK. **Perspectives on holoprosencephaly: part II.** *J Craniofac Genet Dev Biol* 1992;12:196–244
9. Cohen MM. **Perspectives on holoprosencephaly: part III.** 1989; 34:271–288
10. Roach E, DeMyer W, Conneally P, Palmer C, Merritt A. **Holoprosencephaly: birth data, genetic and demographic analysis of 30 families.** *Birth Defects: Original Article Series* 1975;11: 294–313
11. Croen LA, Shaw GM, Lammer EJ. **Holoprosencephaly: epidemiologic and clinical characteristics of a California population.** *Am J Med Genet* 1996;64:465–472
12. Barkovich AJ, Quint DJ. **Middle interhemispheric fusion: an unusual variant of holoprosencephaly.** *AJNR Am J Neuroradiol* 1993;14:431–440
13. Barkovich AJ. ***Pediatric Neuroimaging.*** 3rd ed. Philadelphia: Lippincott Williams & Wilkins; 1999:318–324
14. Golden JA. **Towards a greater understanding of the pathogenesis of holoprosencephaly.** *Brain Dev* 1999;21:513–521
15. Golden J. **Holoprosencephaly: a defect in brain patterning.** *J Neuropathol Exp Neurobiol* 1998;57:991–999
16. Norman M, McGillivray B, Kalousek D, Hill A, Poskitt K. ***Congenital Malformations of the Brain: Pathological, Embryological, Clinical, Radiological and Genetic Aspects.*** New York: Oxford University Press; 1995:187–221
17. Briscoe J, Sussel L, Serup P, et al. **Homeobox gene Nkx2.2 and specification of neuronal identity by graded Sonic hedgehog signaling.** *Nature* 1999;398:622–627
18. Rubenstein JL, Beachy PA. **Patterning of the embryonic forebrain.** *Curr Opin Neurobiol* 1998;8:18–26
19. Belloni E, Muenke M, Roessler E, et al. **Identification of Sonic hedgehog as a candidate gene responsible for holoprosencephaly.** *Nat Genet* 1996;14:353–356
20. Roessler E, Belloni E, Gaudenz K, et al. **Mutations in Sonic hedgehog gene cause holoprosencephaly.** *Nat Genet* 1996;14: 357–360

21. Chiang C, Litingtung Y, Lee E, et al. **Cyclopia and defective axial patterning in mice lacking Sonic hedgehog gene function.** *Nature* 1996;383:407–413
22. Golden JA, Bracilovic A, McFadded KA, et al. **Ectopic bone morphogenetic proteins 5 and 4 in the chicken forebrain lead to cyclopia and holoprosencephaly.** *Proc Natl Acad Sci* 1999; 96:2439–2444
23. Bulfone A, Puelles L, Porteus MH, Frohman MA, Martin GR, Rubenstein JLR. **Spatially restricted expression of Dlx-1, Dlx-2 (Tes-1), Gbx-2, and Wnt-3 in the embryonic day 12.5 mouse forebrain defines potential transverse and longitudinal segmental boundaries.** *J Neurosci* 1993;13:3155–3172
24. Shimamura K, Hartigan DJ, Martinez S, Puelles L, Rubenstein JLR. **Longitudinal organization of the anterior neural plate and neural tube.** *Development* 1995;21:3923–3933
25. Rubenstein JL, Shimamura K, Martinez S, Puelles L. **Regionalization of the prosencephalic neural plate.** *Annu Rev Neurosci* 1998;21:445–477
26. Puelles L, Rubenstein JLR. **Expression patterns of homeobox and other putative regulatory genes in the embryonic mouse forebrain suggest a neuromeric organization.** *Trends Neurosci* 1995;16:472–479
27. Brown SA, Warburton D, Brown LY, et al. **Holoprosencephaly due to mutations in ZIC2, a homologue of Drosophila oddpaired.** *Nat Genet* 1998;20:180–183
28. Wallis DE, Roessler E, Hehr U, et al. **Mutations in the homeodomain of the human SIX3 gene cause holoprosencephaly.** *Nat Genet* 1999;22:196–198
29. Roessler E, Muenke M. **Holoprosencephaly: a paradigm for the complex genetics of brain development.** *J Inherit Metab Dis* 1998;21:481–497